
Figures and figure supplements

SOD1 is a synthetic-lethal target in *PPM1D*-mutant leukemia cells

Linda Zhang et al.

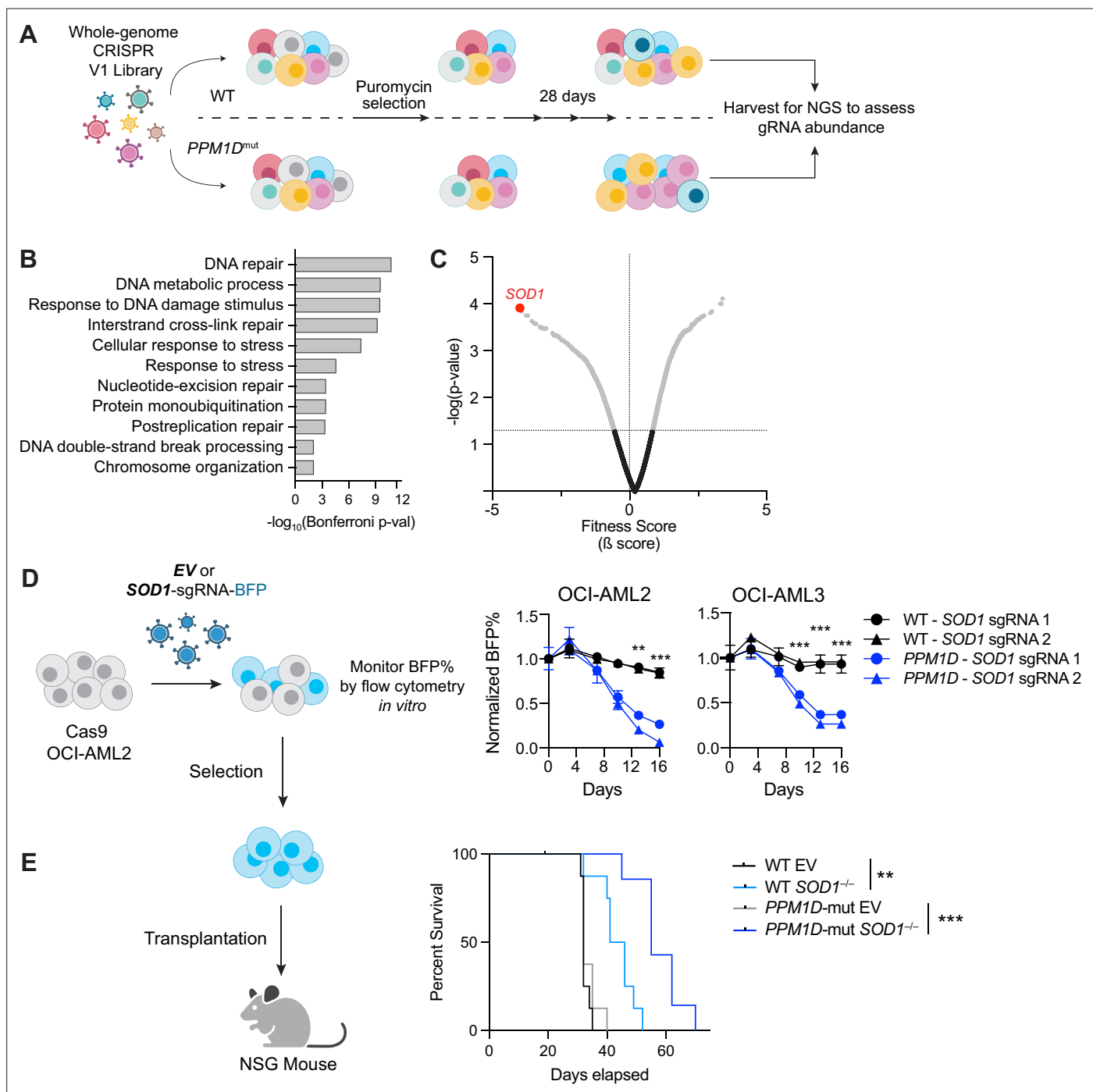


Figure 1. *SOD1* is a synthetic-lethal vulnerability of *PPM1D*-mutant leukemia cells. **(A)** Schematic of whole-genome CRISPR dropout screen. Wild-type (WT) Cas9-expressing OCI-AML2 and two isogenic *PPM1D*-mutant lines were transduced with the Human Improved Whole Genome Knockout CRISPR library V1 containing 90,709 guide RNAs (gRNAs) targeting 18,010 human genes at low multiplicity of infection (MOI~0.3). Each condition was performed in technical triplicates. Three days post-transduction, cells underwent puromycin selection for 3 days. Cells were harvested at day 10 as the initial timepoint and then harvested every 3 days afterward. sgRNA-sequencing was performed on cells collected on day 28. **(B)** Top biological processes based on gene ontology analysis of the top 37 genes essential for *PPM1D*-mutant cell survival. Enrichment and depletion of guides and genes were analyzed using MAGeCK-VISPR by comparing read counts from each *PPM1D*-mutant cell line replicate with counts from the initial starting population at day 10. **(C)** Volcano plot of synthetic-lethal hits ranked by fitness score with a negative score indicating genes for which their knockout leads to decreased growth or survival. *SOD1* (highlighted) was the top hit from the screen. **(D)** Left: Schematic of competitive proliferation assays used for validation of CRISPR targets. Right: WT and *PPM1D*-mutant Cas9-OCI-AML2 and Cas9-OCI-AML3 cells were transduced with lentiviruses containing a single *SOD1*-gRNA with a blue fluorescent protein (BFP) reporter. Cells were assayed by flow cytometry every 3–4 days and normalized

Figure 1 continued on next page

Figure 1 continued

to the BFP percentage at day 3 post-transduction. Two unique gRNAs against *SOD1* were used per cell line and each condition was performed in technical duplicates; multiple unpaired t-tests, ** $p < 0.01$, *** $p < 0.001$. (E) Left: Cas9-expressing WT and *PPM1D*-mutant cells were transduced with control or sg*SOD1*-containing lentiviruses and underwent puromycin (3 $\mu\text{g/mL}$) selection for 3 days prior to transplantation. Sublethally irradiated (250 cGy) NSG mice were intravenously transplanted with 3×10^6 cells. Right: Kaplan-Meier survival curve of mice transplanted with WT or *PPM1D*-mutant (gray) leukemia cells with or without *SOD1* deletion. The median survival of mice transplanted with WT, WT/*SOD1*^{-/-}, *PPM1D*^{mut}, and *PPM1D*^{mut}/*SOD1*^{-/-} leukemia cells was 32, 43, 32, and 55 days, respectively; Mantel-Cox test, ** $p < 0.01$, *** $p < 0.001$.

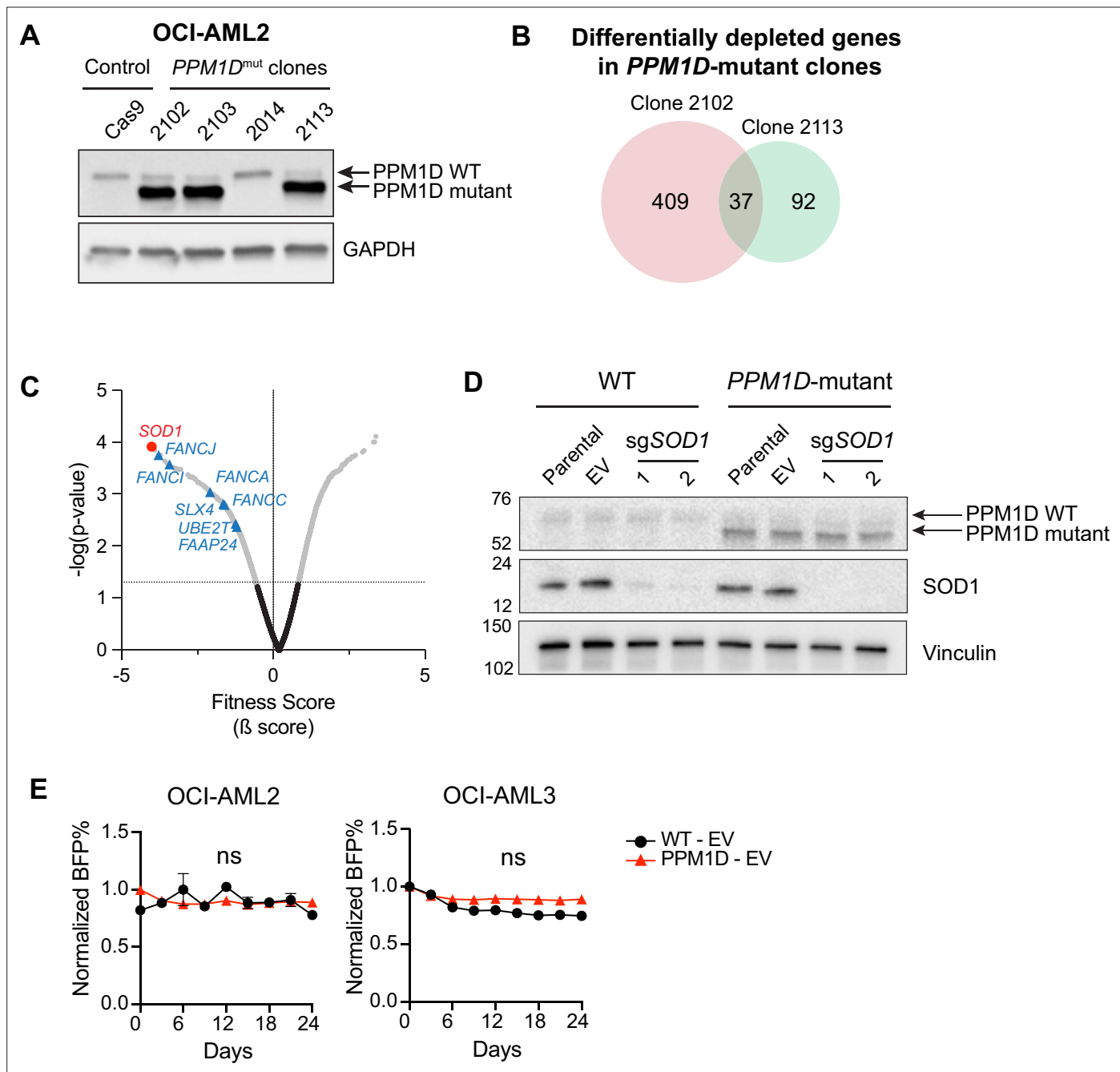


Figure 1—figure supplement 1. *SOD1* is a synthetic-lethal vulnerability of *PPM1D*-mutant leukemia cells. **(A)** Immunoblot validation of *PPM1D*-mutant Cas9-expressing OCI-AML2 cells generated and used for CRISPR screening. Blots were probed with anti-PPM1D (1:1000) and GAPDH (1:1000). Clones 2102 and 2113 were selected for the dropout screen. **(B)** Venn diagram of genes that were depleted from the two *PPM1D*-mutant clones (#2102, 2113) used in the dropout screen, but not depleted in the wild-type (WT) control lines. 37 genes were found to be depleted in both mutant clones. For a full list of genes, see **Figure 1—source data 1**. **(C)** Volcano plot of synthetic-lethal hits ranked by fitness score with the Fanconi anemia pathway genes highlighted in blue. **(D)** Immunoblot validation of *SOD1* deletion. WT and *PPM1D*-mutant Cas9-OCI-AML2 cells were transduced with control (empty vector [EV]) or sg*SOD1* lentiviruses. Two sgRNAs targeting *SOD1* were tested. Three days post-transduction, the cells underwent puromycin selection (3 μ g/mL) for 3 days after which they were harvested for western blot. Blots were probed with anti-PPM1D (1:1000), anti-SOD1 (1:500), and anti-vinculin (1:2500). **(E)** Cas9-OCI-AML2 and Cas9-OCI-AML3 WT or *PPM1D*-mutant cells were transduced with the empty vector control backbone tagged with a blue fluorescent protein (BFP) reporter. Cells were assayed by flow cytometry between 3 and 24 days post-transduction and normalized to the BFP percentage at day 3. Data shown are mean \pm SD (n=2 per condition).

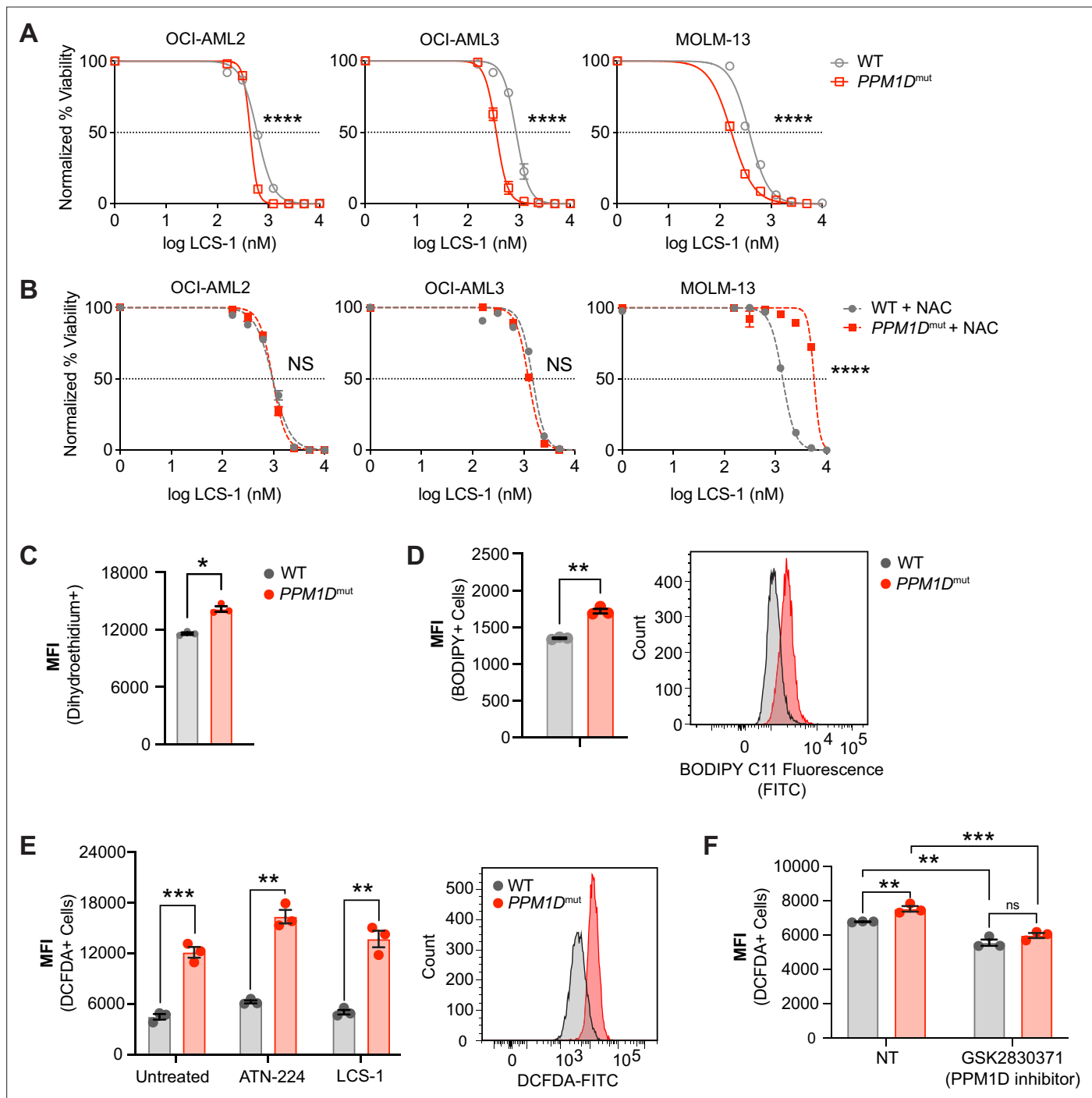


Figure 2. *PPM1D*-mutant cells are sensitive to SOD1 inhibition and have increased oxidative stress. (A,B) Dose response curves for cell viability with SOD1-inhibitor (LCS-1) (A) or LCS-1 in combination with 0.25 μ M NAC (B) in WT and *PPM1D*-mutant leukemia cell lines after 24-hours. Mean \pm SD (n=3) is shown with a non-linear regression curve. All values are normalized to the baseline cell viability with vehicle, as measured by MTT assay. (C) Endogenous cytoplasmic superoxide levels of WT and *PPM1D*-mutant leukemia cell lines were measured using dihydroethidium (5 μ M). The mean fluorescence intensity (MFI) of dihydroethidium was measured by flow cytometry. Mean \pm SD (n=3) is shown. (D) Lipid peroxidation measured using BODIPY 581/591 staining (2.5 μ M) of WT and *PPM1D*-mutant OCI-AML2 cells. The MFI was measured by flow cytometry. Mean \pm SD (n=3) is shown. (E-F) Measure of total reactive oxygen species using 2',7'-dichlorofluorescein diacetate (DCFDA) staining (10 μ M) measured by flow cytometry. WT and *PPM1D*-mutant OCI-AML2 cells were measured at baseline and 24-hrs after SOD1 inhibition (ATN-224 12.5 μ M, LCS-1 0.625 μ M) (E) or 24-hrs after pharmacologic *PPM1D* inhibition (GSK2830371, 5 μ M) (F); unpaired t-tests were used for statistical analyses, ns=non-significant (p>0.05), **p<0.01, ***p<0.001, ****p<0.0001.

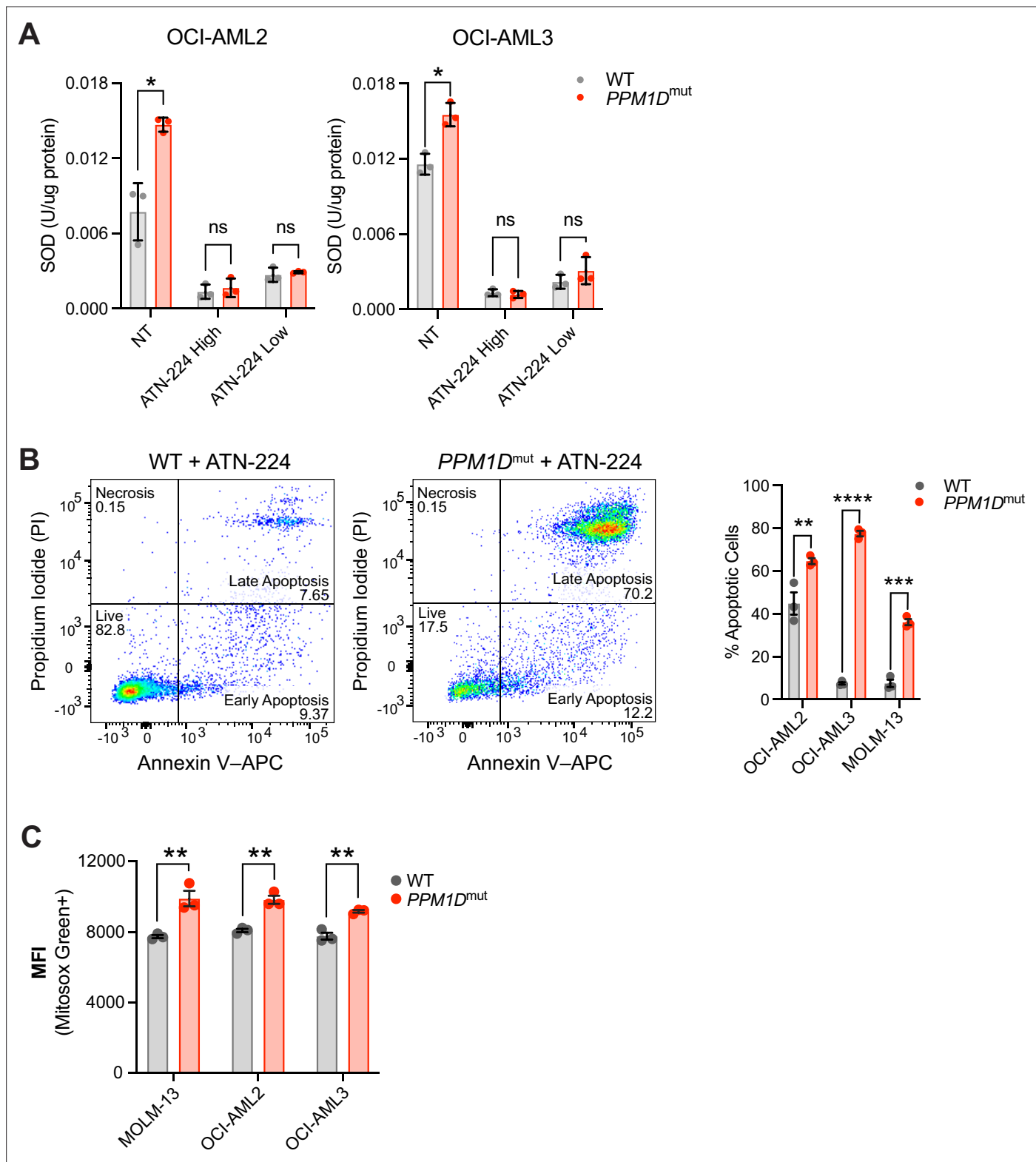


Figure 2—figure supplement 1. *PPM1D*-mutant cells have increased oxidative stress. **(A)** Superoxide dismutase (SOD) activity assays in OCI-AML2 and OCI-AML3 cells at baseline (NT), or treated with high (12.5 μ M) or low (6.25 μ M) doses of ATN-224 for 16 hr. **(B)** Left: Representative flow cytometry plots of wild-type (WT) and *PPM1D*-mutant cells treated with ATN-224 (25 μ M for 24 hr) and stained for Annexin V-APC and PI for apoptosis; multiple unpaired t-tests, ns = non-significant, * $p < 0.05$, ** $p < 0.01$, *** $p < 0.001$, **** $p < 0.0001$. **(C)** Endogenous mitochondrial superoxide levels of WT and *PPM1D*-mutant leukemia cell lines were measured using MitoSOX Green staining (1 μ M). The mean fluorescence intensity (MFI) of MitoSOX Green was measured by flow cytometry. Mean \pm SD ($n = 3$) is shown.

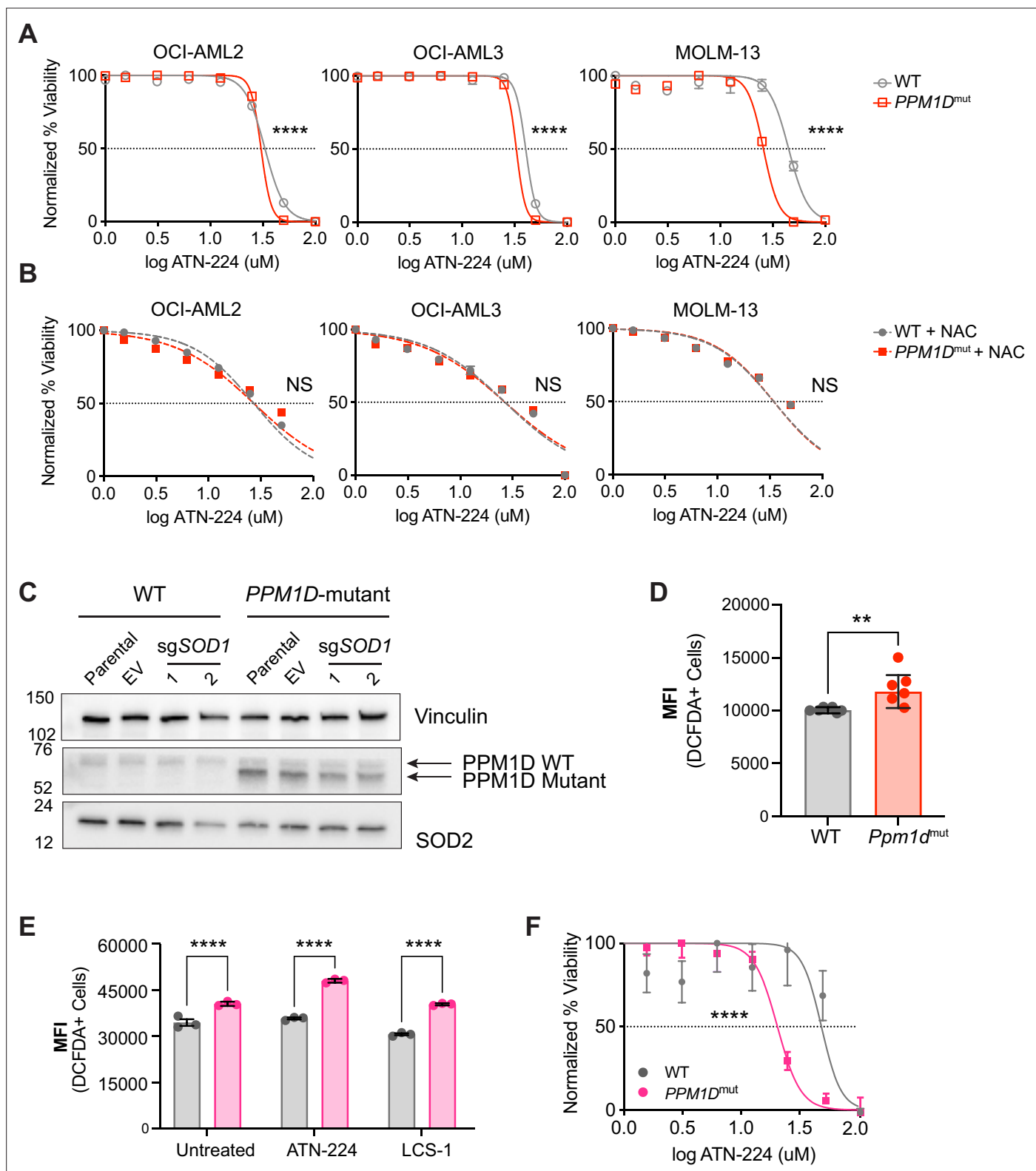


Figure 2—figure supplement 2. *PPM1D*-mutant cells have increased oxidative stress. (A,B) Dose-response curves for cell viability with SOD1 inhibitor (ATN-224) (A) or ATN-224 in combination with 0.25μM N-acetylcysteine (NAC) (B) in wild-type (WT) and *PPM1D*-mutant leukemia cell lines after 24hr. Mean ± SD (n=3) is shown along with a non-linear regression curve. All values are normalized to the baseline cell viability with vehicle, as measured by MTT assay. (C) Immunoblot of SOD2 expression in WT and *PPM1D*-mutant cells at baseline and after SOD1 deletion. WT and *PPM1D*-mutant Cas9-OCI-AML2 cells were transduced with control (empty vector [EV]) or sgSOD1 lentiviruses. Two sgRNAs targeting SOD1 were tested. Three days

Figure 2—figure supplement 2 continued on next page

Figure 2—figure supplement 2 continued

post-transduction, the cells underwent puromycin selection (3 $\mu\text{g}/\text{mL}$) for days after which they were harvested for western blot. Blots were probed with anti-PPM1D (1:1000), anti-SOD2 (1:1000), and anti-vinculin (1:2500). **(D)** Total reactive oxygen species (ROS) of WT and Ppm1d-mutant mouse embryonic fibroblasts (MEFs) measured by 2',7'-dichlorofluorescein diacetate (DCFDA) (10 μM) staining. Mean fluorescence intensity (MFI) was determined by flow cytometry. $n=6$ biological replicates were used for each genotype. Data shown are the mean of each biological replicate; unpaired t-test. **(E)** Total ROS of WT GM12878 (gray) and PPM1D-mutant (pink) patient lymphoblastoid cell lines (LCLs) at baseline and after 24 hr of SOD1 inhibition measured by DCFDA (10 μM) staining. MFI was determined by flow cytometry; multiple unpaired t-tests. **(F)** Dose-response curve of WT and PPM1D-mutant LCLs after ATN-224 treatment. IC50s of WT and PPM1D-mutant LCLs were 48.8 μM and 20.51 μM , respectively, as measured by MTT assay; non-linear regression analysis, ns = non-significant ($p>0.05$), ** $p<0.01$, *** $p<0.001$, **** $p<0.0001$.

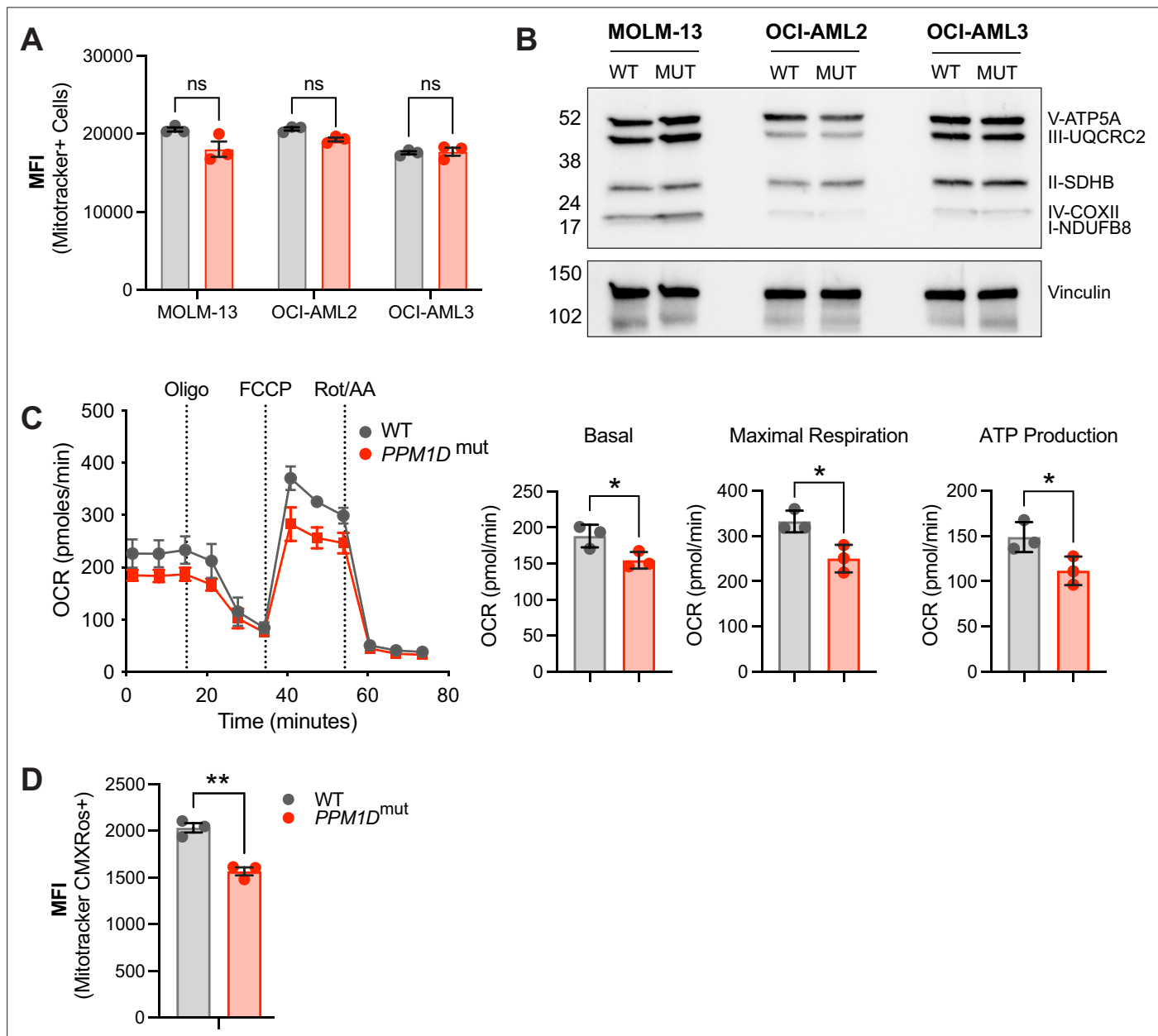


Figure 3. *PPM1D*-mutant cells have altered mitochondrial function. **(A)** Mitochondrial mass of wild-type (WT) and *PPM1D*-mutant leukemia cells was determined using MitoTracker Green (100 nM) and the mean fluorescence intensity was analyzed by flow cytometry. Data represents mean \pm SD of triplicates. At least three independent experiments were conducted with similar findings; unpaired t-tests. **(B)** Immunoblot of WT and *PPM1D*-mutant cell lysates probed with the human OXPHOS antibody cocktail (1:1000) and vinculin (1:2000). **(C)** Measurement of mitochondrial oxygen consumption rate (OCR) by seahorse assay in WT and *PPM1D*-mutant OCI-AML2 cells after treatment with oligomycin (1.5 μ M), FCCP (0.5 μ M), and rot/AA (0.5 μ M). Quantification of basal, maximal, and ATP-linked respiration are shown. Data shown are the mean \pm SD of technical triplicates. **(D)** Mitochondrial membrane potential of WT and *PPM1D*-mutant OCI-AML2 cells was measured using MitoTracker CMXRos (400 nM). The mean fluorescence intensity (MFI) was measured and analyzed by flow cytometry. Data represents mean \pm SD of triplicates, unpaired t-test, ns = non-significant ($p > 0.05$), * $p < 0.05$, ** $p < 0.01$.

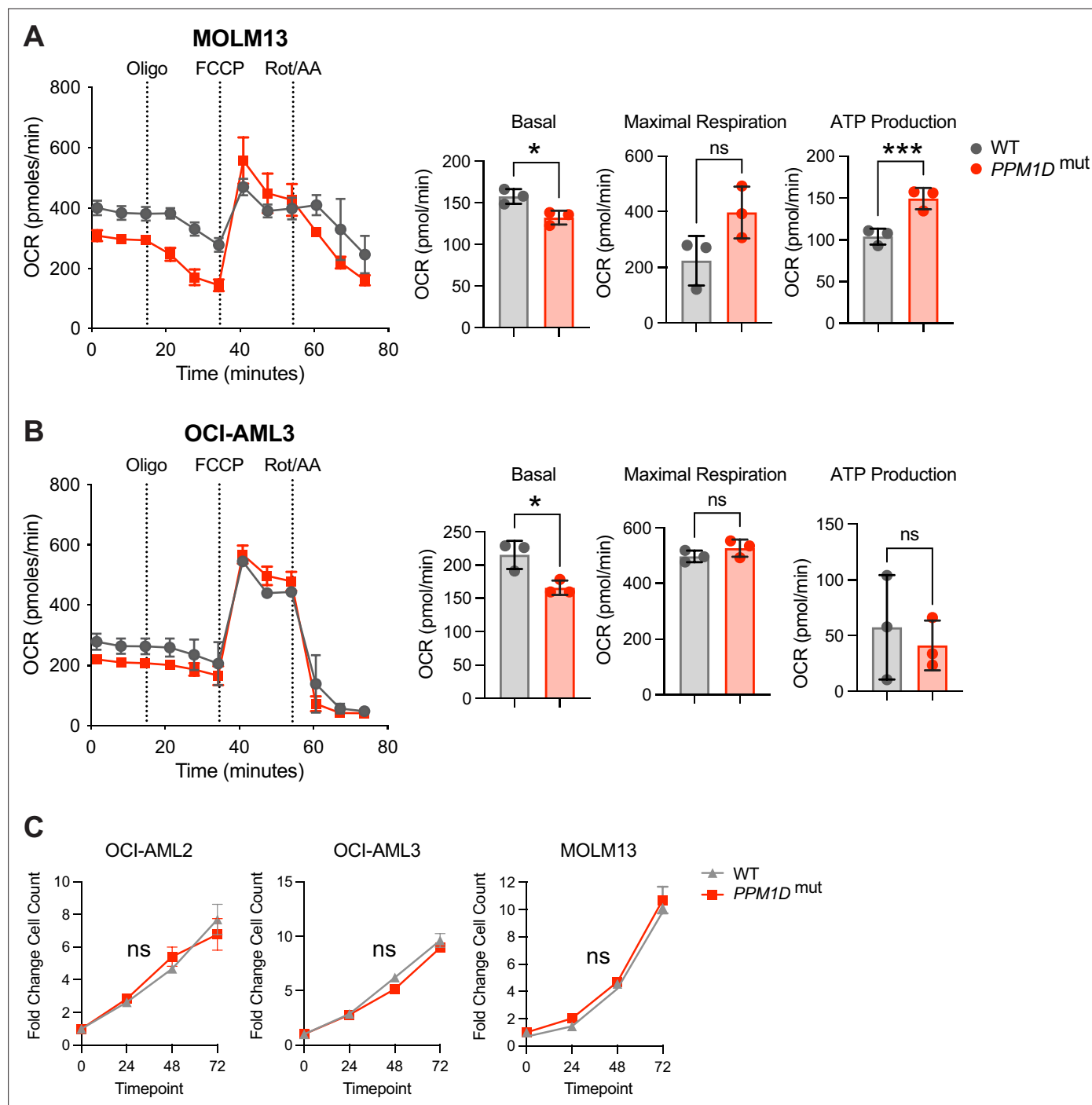


Figure 3—figure supplement 1. *PPM1D*-mutant cells have altered mitochondrial function. (A,B) Measurement of mitochondrial oxygen consumption rate (OCR) by seahorse assay in wild-type (WT) vs. *PPM1D*-mutant MOLM-13 (A) and OCI-AML3 (B) cells after treatment with oligomycin (1.5 μ M), FCCP (0.5 μ M), and rot/AA (0.5 μ M). Quantification of basal, maximal, and ATP-linked respiration shown. Each cell line was performed in technical triplicates, Student's t-test. (C) Growth curves of WT and *PPM1D*-mutant leukemia cell lines at 24, 48, and 72 hr. Cell counts were normalized to day 0. ns = non-significant ($p > 0.05$), * $p < 0.05$, *** $p < 0.001$.

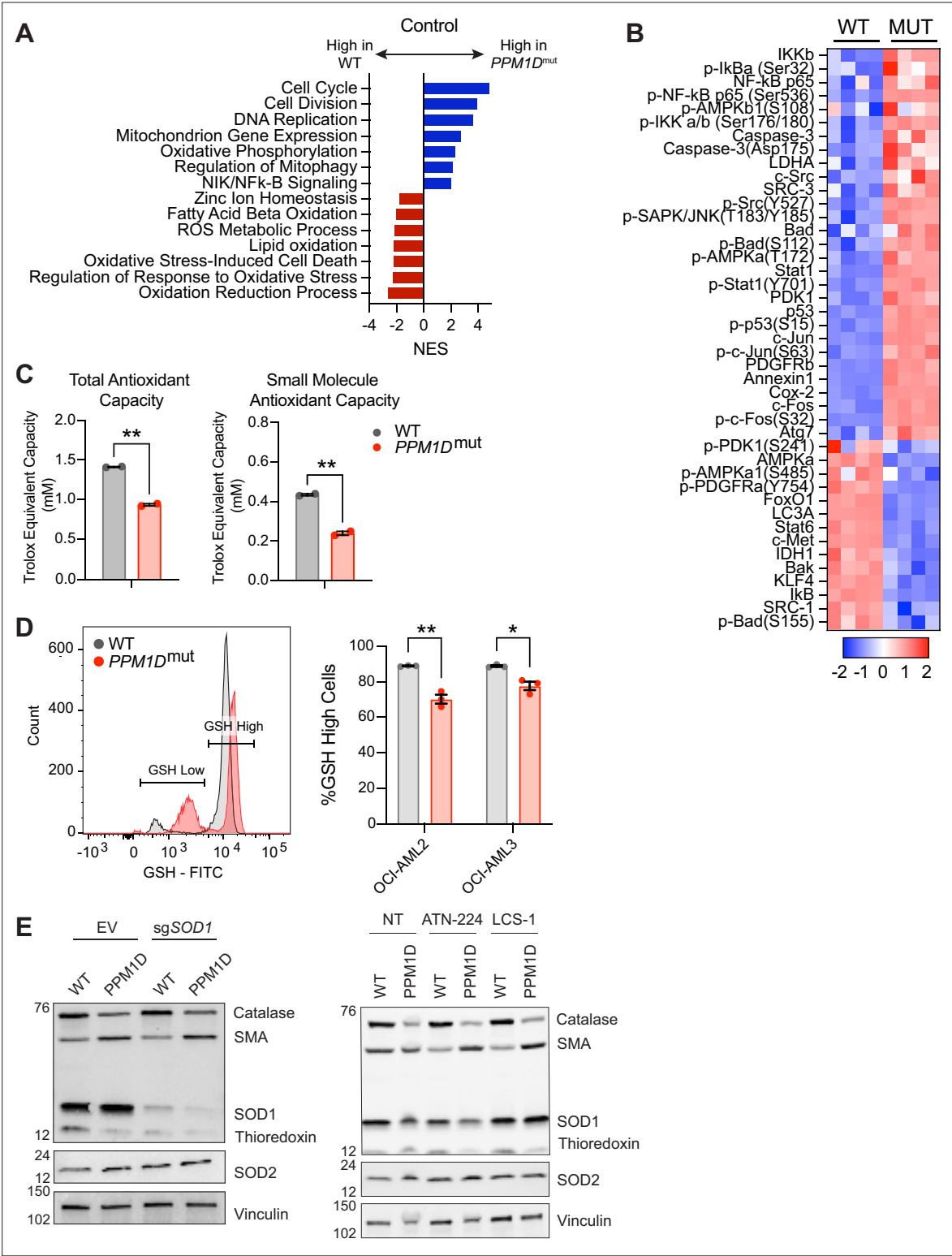


Figure 4. *PPM1D*-mutant cells have a reduced oxidative stress response. **(A)** RNA-sequencing (RNA-seq) gene set enrichment analysis (GSEA) of *PPM1D*-mutant cells compared to wild-type (WT) Cas9-OCI-AML2 cells. Significantly up- and downregulated pathways are indicated by the blue and red bars, respectively. Normalized enrichment scores (NES) are shown with false discovery rate (FDR) < 0.25. **(B)** Reverse-phase protein array (RPPA) profiling of WT and *PPM1D*-mutant OCI-AML2 cells. Proteins from the ‘Response to Oxidative Stress’ pathway have been selected for the heatmap. Each column represents a technical replicate. See **Figure 4—source data 2** for the raw data. **(C)** Total- and small-molecule antioxidant capacity of WT and *PPM1D*-mutant cells performed in technical duplicates. **(D)** Intracellular glutathione (GSH) levels measured by flow cytometry using the Intracellular

Figure 4 continued on next page

Figure 4 continued

GSH Detection Assay Kit (Abcam). Left: Representative flow cytometry plot demonstrating the gating for GSH-high and GSH-low populations. Right: Quantification of the percentage of GSH-high cells for each cell line. Mean \pm SEM (n=3) are shown. **(E)** Immunoblot of WT and *PPM1D*-mutant OCI-AML2 after transduction with the empty vector (EV) control and after *SOD1* deletion (left) or after treatment with SOD1 inhibitors for 16 hr (right, ATN-224 12.5 μ M, lung cancer screen-1 [LCS-1] 1.25 μ M). Lysates were probed with an anti-oxidative stress defense cocktail (1:250), SOD2 (1:1000), and vinculin (1:2000). SMA = smooth muscle actin. Student's t-tests were used for statistical analysis; **p<0.01, *p<0.05.

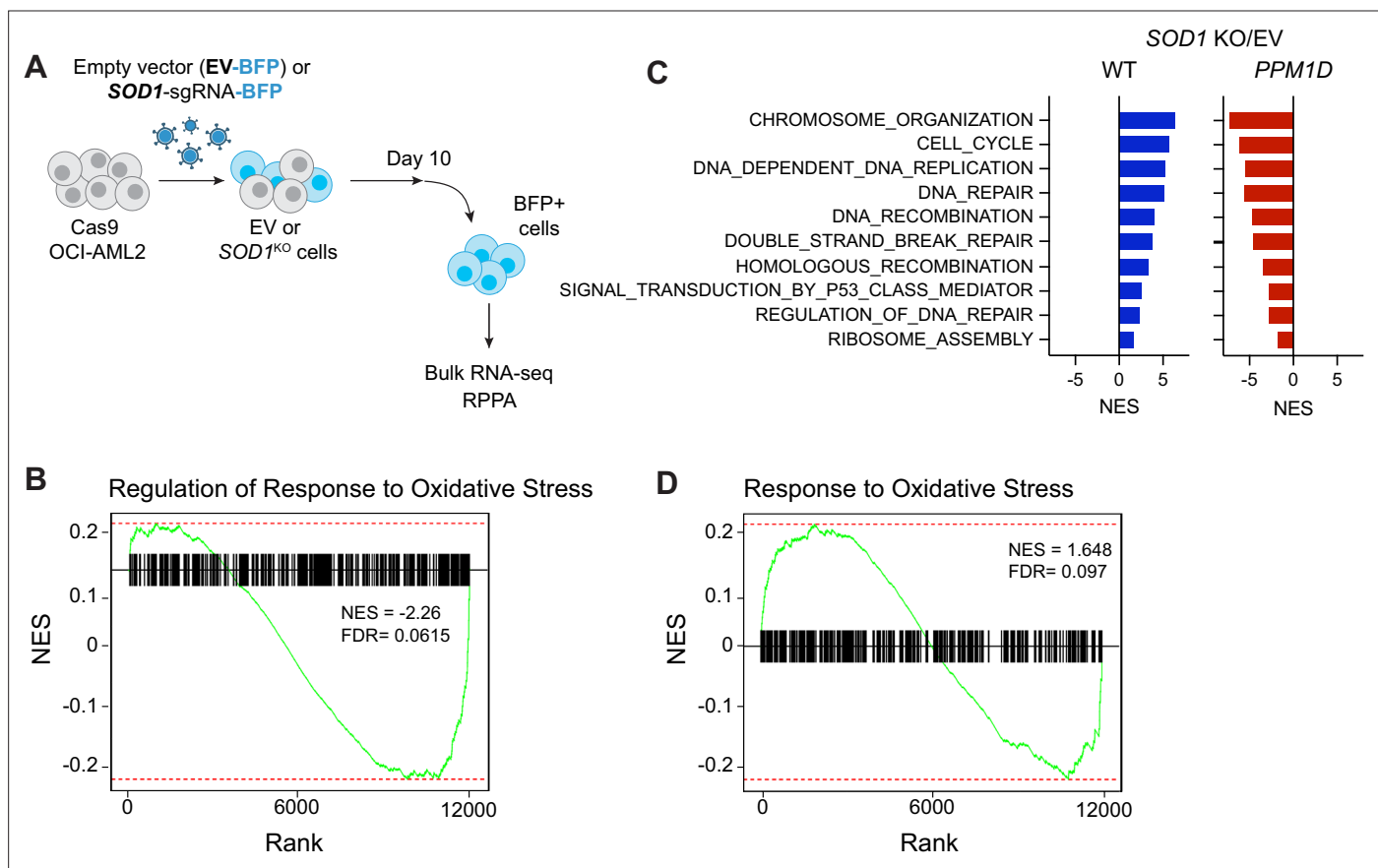


Figure 4—figure supplement 1. *PPM1D*-mutant cells have reduced oxidative stress response. **(A)** Schematic of the experimental setup for the bulk RNA-sequencing and reverse-phase protein array. Wild-type (WT) and *PPM1D*-mutant Cas9 OCI-AML2 cells were transduced with either empty vector (EV)-blue fluorescent protein (BFP) or *SOD1*-sgRNA-BFP. Cells were passaged for 10 days and then sorted for BFP expression for downstream analysis. **(B, D)** Gene set enrichment analysis (GSEA) enrichment plots for *PPM1D*-mutant cells compared to WT after transduction with EV **(B)** or after *SOD1*-knockout **(D)** for the 'Regulation of Response to Oxidative Stress' (GO:1902882) and 'Response to Oxidative Stress' (GO:0006979). Normalized enrichment scores (NES) are shown with false discovery rate (FDR) < 0.25. **(C)** GSEA of RNA-sequencing of *SOD1*-deleted cells compared to EV control in WT and *PPM1D*-mutant cells. Blue and red bars indicate significantly up- and downregulated pathways, respectively. NES are indicated. All pathways filtered for FDR < 0.25. See **Figure 4—source data 1** for raw data.

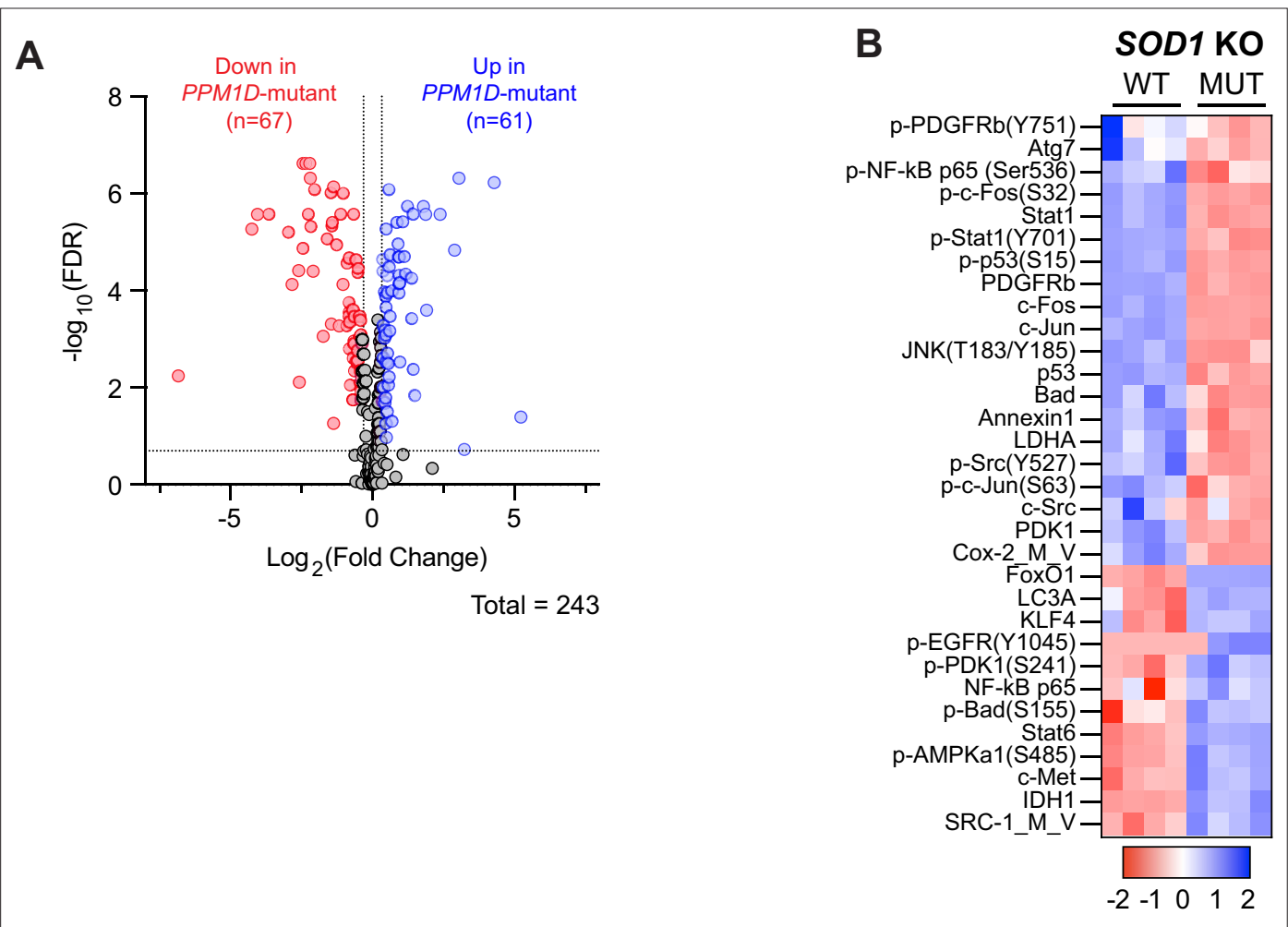


Figure 4—figure supplement 2. *PPM1D*-mutant cells have reduced oxidative stress response. **(A)** Volcano plot of the differentially expressed proteins from the reverse-phase protein array (RPPA) in *PPM1D*-mutant OCI-AML2 cells compared to wild-type (WT). Red and blue dots indicate significantly up- and downregulated proteins, respectively, with a cutoff false discovery rate (FDR) < 0.2 and linear fold change > |1.2|. **(B)** RPPA profiling of WT and *PPM1D*-mutant cells after *SOD1* deletion. Proteins from the ‘Response to Oxidative Stress’ pathway have been selected for the heatmap. Each column represents a technical replicate. See **Figure 4—source data 2** for the raw data.

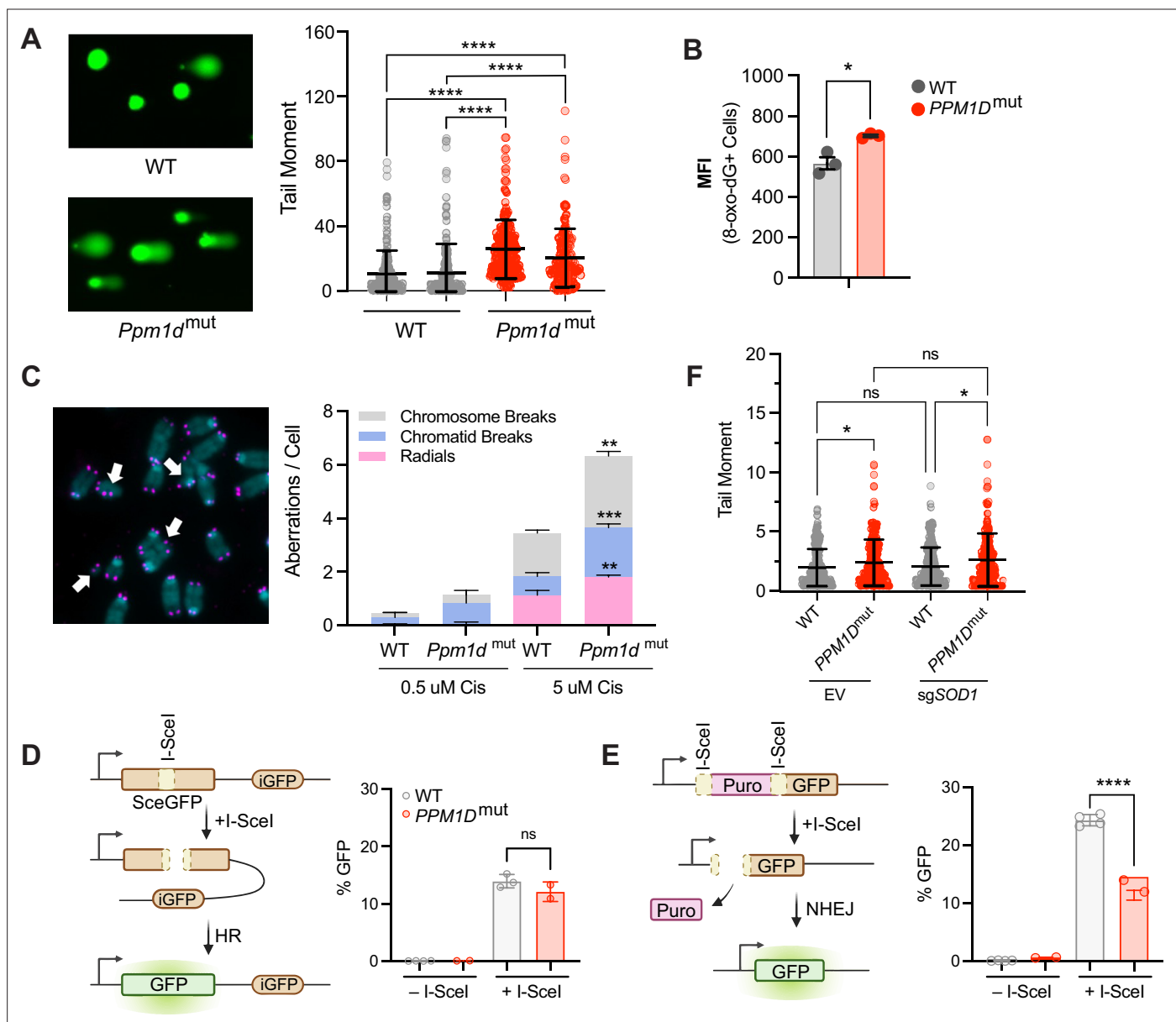


Figure 5. *PPM1D* mutations increase genomic instability and impair non-homologous end-joining. (A) Left: Representative images of comet assays of mouse embryonic fibroblasts (MEFs). Two biological replicates were assessed for each genotype. Right: Quantification of $n \geq 150$ comets per experimental group with the Comet IV software; two-way ANOVA. (B) Mean fluorescent intensity (MFI) of 8-oxo-2'-deoxyguanosine (8-oxo-dG) lesions within wild-type (WT) and *PPM1D*-mutant OCI-AML2 cells as measured by flow cytometry; Student's t-test. (C) Left: Representative images of metaphase spreads of WT and *Ppm1d*-mutant mouse primary B-cells treated with low (0.5 μM) or high (5 μM) doses of cisplatin. Right: $n \geq 50$ metaphase cells were quantified in each experimental condition for chromosomal aberrations (white arrows). $n = 2$ biological replicates used for each genotype. Student's t-test was used for statistical analysis. (D–E) Left: Schematic of the homologous recombination (D) or non-homologous end-joining (E) U2OS DNA damage repair cassettes. Right: Quantification of GFP% analyzed by flow cytometry 48 hr after induction of DNA damage by I-SceI transduction; Student's t-test. (F) Comet assay quantification of WT and *PPM1D*-mutant Cas9-OCI-AML2 cells 6 days after lentiviral transduction with the empty vector (EV) control, or *sgSOD1* to induce *SOD1* deletion. Quantification and analyses of tail moments were performed using the Comet IV software. $n \geq 150$ comets were scored per experimental group; two-way ANOVA. Data are mean \pm SD ($n = 3$), ns = non-significant ($p > 0.05$), * $p < 0.05$, ** $p < 0.01$, *** $p < 0.001$, **** $p < 0.0001$.

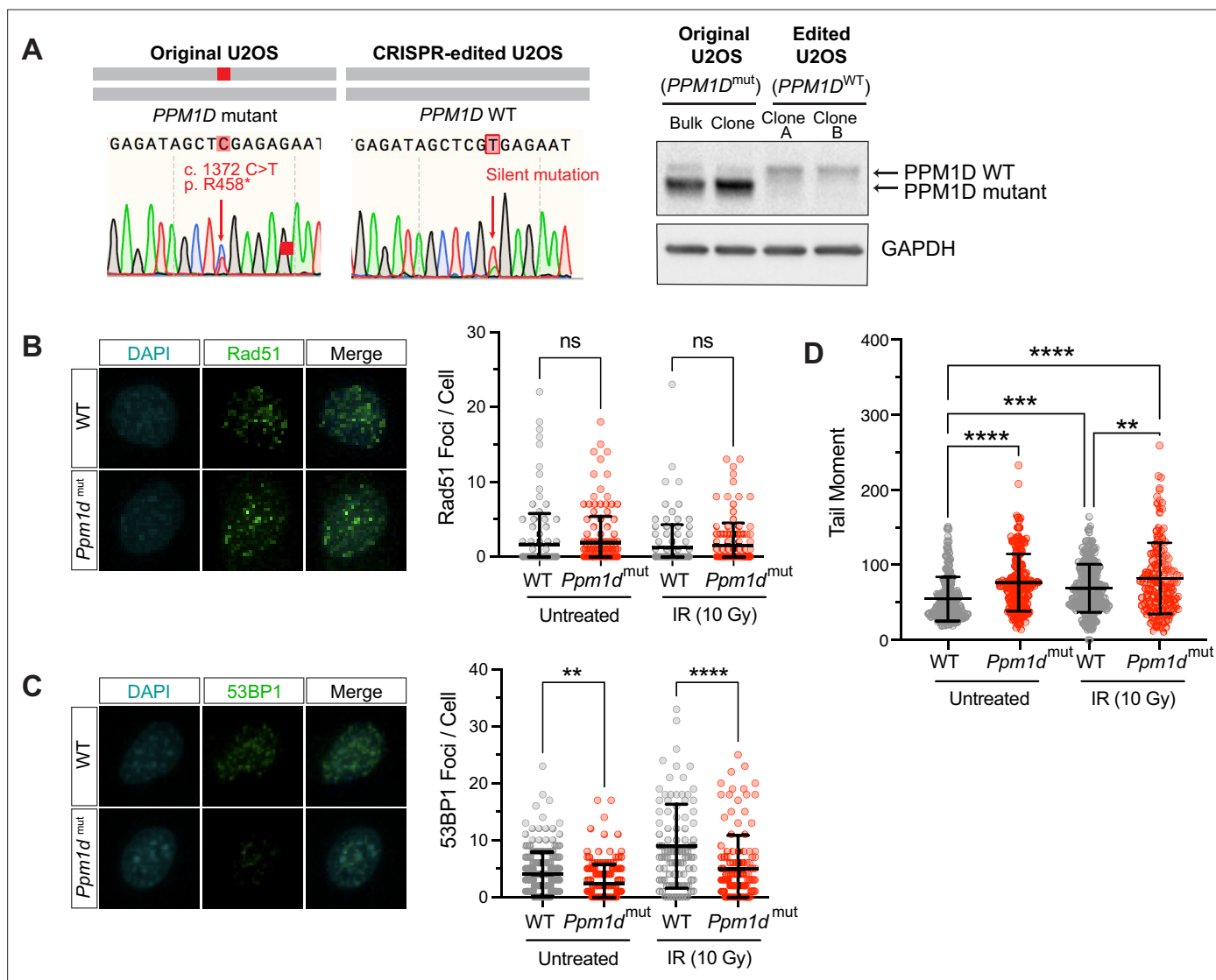


Figure 5—figure supplement 1. *PPM1D*-mutations increase genomic instability and impairs non-homologous end-joining repair. **(A)** Left: Sanger sequencing traces of the parental U2OS cell line harboring a c.1372 C>T mutation in *PPM1D* and the CRISPR-edited U2OS cell line with mutation corrected to wild-type (WT) *PPM1D*. Right: Immunoblot validation of these clones are shown. Lysates were probed with anti-*PPM1D* (1:1000) and anti-GAPDH (1:1000). **(B,C)** Left: Representative images of Rad51 and 53BP1 immunofluorescence microscopy. Mouse embryonic fibroblasts were treated with 10 Gy irradiation, harvested 1 hr post-irradiation and stained for the indicated markers. Right: Quantification of the number of foci per cell is shown. Analysis was performed using CellProfiler. $n > 100$ cells for each condition; Student's t-test. **(D)** Comet assay quantification of mouse embryonic fibroblasts at baseline and after 1 hr post-irradiation (10 Gy). Quantification and analyses of tail moments were performed using the Comet IV software. $n \geq 150$ comets were scored per experimental group; two-way ANOVA, ns = non-significant ($p > 0.05$), * $p < 0.05$, ** $p < 0.01$, *** $p < 0.001$, **** $p < 0.0001$.